The Omicron Variant Increases the Interactions of SARS-CoV-2 Spike Glycoprotein with ACE2

Mert Golcuk[1], *Ahmet Yildiz*[2,3], *Mert Gur*[1*]

[1] Department of Mechanical Engineering, Istanbul Technical University (ITU), 34437, Istanbul, Turkey

[2] Physics Department, University of California, 94720, Berkeley, CA, USA

[3] Department of Molecular and Cell Biology, University of California, 94720, Berkeley, CA, USA

* Corresponding Author; e-mail: gurme@itu.edu.tr

Abstract

The Omicron variant (B.1.1.529) comprises 30 mutations on the spike glycoprotein (S), 15 of which are located on its receptor-binding domain ($RBD_{Omicron}$). RBD interacts with the peptidase domain (PD) of angiotensin-converting enzyme 2 (ACE2) receptors and plays a critical role in the host cell entry of the virus. We performed all-atom simulations of the $RBD_{Omicron}$-PD in the presence of explicit water and ions. Simulations showed a considerably more extensive interactions network between $RBD_{Omicron}$ and PD compared to RBD_{WT}, comprising a 250%, 10% and -25% change in the total number of salt bridges, hydrophobic interactions, hydrogen bonds at the S-ACE2 interface, respectively. Using the conformations sampled in each our MD trajectories, binding energies of two sets of RBD_{WT}-PD and four sets of $RBD_{Omicron}$-PD simulations were calculated via the Molecular Mechanics Poisson-Boltzmann Surface Area (MMPBSA) method, estimating ~44% stronger binding energy for $RBD_{Omicron}$ compared to RBD_{WT}. Our results suggest that an increase in the number of salt bridges in the S-ACE2 interface result in a higher binding strength of RBD to PD, which may result in a higher efficiency of the SARS-CoV-2 virus to infect host cells. Furthermore, $RBD_{Omicron}$ exhibits a more dispersed interaction network on both sides of the RBD-PD interaction surface compared to WT.

The recent appearance and the rapid rate of infection of a heavily mutated B.1.1.529 variant of SARS-CoV-2, named Omicron, have raised concerns around the world, with many countries limiting their international travel. This variant comprises 30 mutations on the spike glycoprotein (S), 15 of which are located on its receptor-binding domain ($RBD_{Omicron}$). RBD interacts with the peptidase domain (PD) of angiotensin-converting enzyme 2 (ACE2) receptors and plays a critical role in the host cell entry of the virus. RBD is a critical antibody and drug target, and all of the available vaccines produce antibodies that neutralize the RBD-PD interaction. Mutations on $RBD_{Omicron}$ are surface-exposed and being targeted by antibodies (Figure S1) and nanobodies. In addition, 11 of these 15 mutations (K417N, N440K, G446S, S477N, T478K, E484A, Q493R, G496S, Q498R, N501Y, Y505H; Figure 1) are located on the ACE2 binding interface. Our previous all-atom Molecular Dynamics (MD) simulations[1] showed that 5 of these residues form pairwise interactions between wild-type (WT) S and ACE2 (salt bridges between K417-D30 and E484-K31 salt bridges, and hydrogen bonding between Q493-E35, Q498-Q42, Q498-K353, and Y505-E37). It remains unclear how these mutations affect the binding strength of $RBD_{Omicron}$ to ACE2 and the ability of existing SARS CoV-2 antibodies to neutralize this interaction.

Here we performed all-atom simulations of the $RBD_{Omicron}$-PD in the presence of explicit water and ions (~200k atoms in total) using NAMD3.[2] Full-length glycans on RBD and ACE2 were included in simulations.[3,4] 4 sets of MD simulations totaling 900 ns in length were performed using parameters identical to our RBD-PD simulations for the WT,[1] alpha, and beta variants.[5] Simulations showed a considerably more extensive interactions network between $RBD_{Omicron}$ and PD compared to RBD_{WT}. We detected seven salt bridges $RBD_{Omicron}$ and PD and the disappearance of the two salt bridges that form between RBD_{WT} and PD. The $RBD_{Omicron}$ forms all of the ten hydrophobic interactions that were observed for RBD_{WT}-PD and forms an additional hydrophobic interaction between Y501-Y41. Compared to eight hydrogen binding between RBD_{WT} and PD, six hydrogen bonds were observed between $RBD_{Omicron}$ and PD. Only one of these interactions was also observed for the WT, while other are newly formed. Collectively, the total number of salt bridges, hydrophobic interactions, hydrogen bonds at the S-ACE2 interface changed by 250%, 10% and -25%, respectively.

Using the conformations sampled in each our MD trajectories, binding energies of two sets of RBD_{WT}-PD and four sets of $RBD_{Omicron}$-PD simulations were calculated via the Molecular Mechanics Poisson-Boltzmann Surface Area (MMPBSA) method[6,7] using the Visual Molecular Dynamics (VMD)[8] plugin CaFE[9] (Table S1). MMPBSA calculations estimated 44% stronger binding energy (-39±6 kcal/mol, average of four sets) for $RBD_{Omicron}$ compared to RBD_{WT} (-27±2.6 kcal/mol, average of two sets). Our results suggest that an increase in the number of salt bridges in the S-ACE2 interface result in a higher binding strength of RBD to PD, which may result in a higher efficiency of the SARS-CoV-2 virus to infect host cells.

Simulations also revealed a change in the distribution of RBD-PD interactions due to the mutations in the Omicron variant. Between RBD_{WT} and PD, salt bridges are concentrated at the interface of contact region 1 (CR1) and CR2, hydrogen bonding are more concentrated in CR3, and hydrophobic interactions are concentrated in CR 1. In comparison, $RBD_{Omicron}$ exhibits a more dispersed interaction network on both sides of the RBD-PD interaction surface (Figure 2). This may result in an altered binding mechanism and negatively impact the current inhibition mechanism by neutralizing antibodies and nanobodies.

$RBD_{Omicron}$ mutations may also affect the binding affinity and neutralizing capability of SARS-CoV-2 S antibodies and nanobodies, such as H11-H4, H11-D4, and Ty1.[5,10,11] For example, we expect E484A mutation to eliminate E484-R52 salt bridge and E484-S57 hydrogen bonds in H11-H4 and H11-D4, and E484-N56, and E484-Y335 hydrogen bonds in Ty1. Additionally, Q493R mutation would eliminate the hydrogen bonds Q493-Y104 and Q493-S104 in H11-H4, and H11-D4, respectively. Future studies are required to determine whether these mutations increase the resistance of the Omicron variant to antibodies.

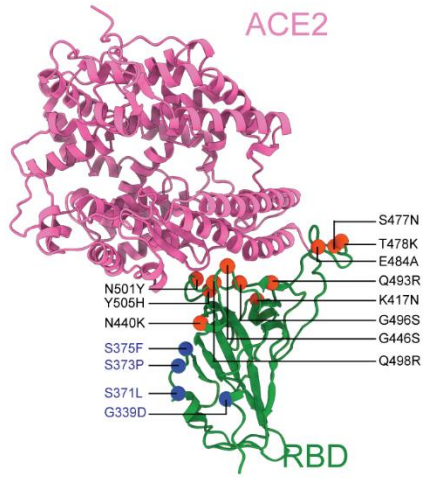

Figure 1 Location of RBD mutations for the Omicron variant.

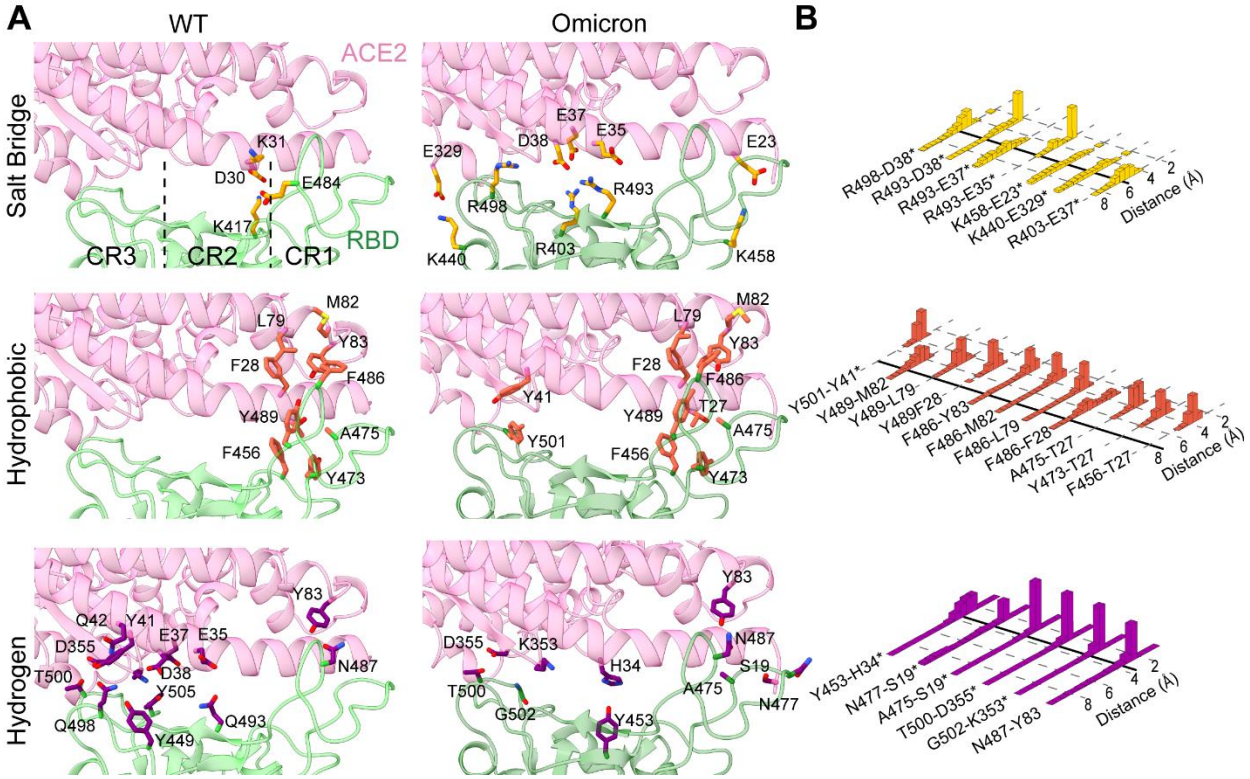

Figure 2. Interactions between $RBD_{Omicron}$ of the SARS-CoV-2 S protein and the PD of human ACE2. (A) Representative snapshots of the all-atom MD simulations highlight salt bridges, hydrophobic interactions, and hydrogen bonding between RBD_{WT}-PD and $RBD_{Omicron}$-PD. The interaction surface is divided into three distinct regions (CR1-3)[1,12] (B) Normalized distributions of the distances between the amino-acid pairs that form salt bridges (orange), hydrophobic interactions (red), and hydrogen bonds (purple) between $RBD_{Omicron}$-PD. Newly formed interactions due to mutations are marked with an asterisk.

Acknowledgements

This work is supported by COVID-19 HPC Consortium (Grant number: TG-BIO200053)

References

1 Taka, E. *et al.* Critical Interactions Between the SARS-CoV-2 Spike Glycoprotein and the Human ACE2 Receptor. *The Journal of Physical Chemistry B* **125**, 5537-5548, doi:10.1021/acs.jpcb.1c02048 (2021).

2 Phillips, J. C. *et al.* Scalable molecular dynamics on CPU and GPU architectures with NAMD. *The Journal of Chemical Physics* **153**, 044130, doi:10.1063/5.0014475 (2020).

3 Casalino, L. *et al.* Beyond Shielding: The Roles of Glycans in the SARS-CoV-2 Spike Protein. *ACS Cent. Sci.* **6**, 1722-1734, doi:10.1021/acscentsci.0c01056 (2020).

4 Barros, E. P. *et al.* The flexibility of ACE2 in the context of SARS-CoV-2 infection. *Biophysical Journal* **120**, 1072-1084, doi:https://doi.org/10.1016/j.bpj.2020.10.036 (2021).

5 Golcuk, M., Hacisuleyman, A., Erman, B., Yildiz, A. & Gur, M. Binding Mechanism of Neutralizing Nanobodies Targeting SARS-CoV-2 Spike Glycoprotein. *Journal of Chemical Information and Modeling* **61**, 5152-5160, doi:10.1021/acs.jcim.1c00695 (2021).

6 Kollman, P. A. *et al.* Calculating Structures and Free Energies of Complex Molecules: Combining Molecular Mechanics and Continuum Models. *Accounts of Chemical Research* **33**, 889-897, doi:10.1021/ar000033j (2000).

7 Srinivasan, J., Cheatham, T. E., Cieplak, P., Kollman, P. A. & Case, D. A. Continuum Solvent Studies of the Stability of DNA, RNA, and Phosphoramidate−DNA Helices. *Journal of the American Chemical Society* **120**, 9401-9409, doi:10.1021/ja981844+ (1998).

8 Humphrey, W., Dalke, A. & Schulten, K. VMD: Visual molecular dynamics. *Journal of Molecular Graphics* **14**, 33-38, doi:https://doi.org/10.1016/0263-7855(96)00018-5 (1996).

9 Liu, H. & Hou, T. CaFE: a tool for binding affinity prediction using end-point free energy methods. *Bioinformatics* **32**, 2216-2218 (2016).

10 Huo, J. *et al.* Neutralizing nanobodies bind SARS-CoV-2 spike RBD and block interaction with ACE2. *Nature Structural & Molecular Biology* **27**, 846-854, doi:10.1038/s41594-020-0469-6 (2020).

11 Hanke, L. *et al.* An alpaca nanobody neutralizes SARS-CoV-2 by blocking receptor interaction. *Nature Communications* **11**, 4420, doi:10.1038/s41467-020-18174-5 (2020).

12 Wang, Y., Liu, M. & Gao, J. Enhanced receptor binding of SARS-CoV-2 through networks of hydrogen-bonding and hydrophobic interactions. *Proceedings of the National Academy of Sciences* **117**, 13967-13974 (2020).

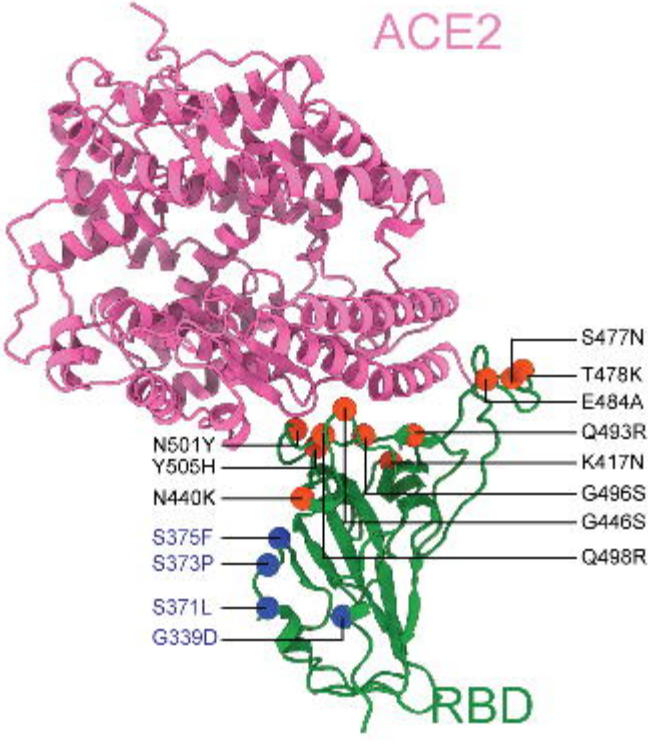
ACE2
S477N
T478K
E484A
Q493R
K417N
G496S
G446S
Q498R
N501Y
Y505H
N440K
S375F
S373P
S371L
G339D
RBD

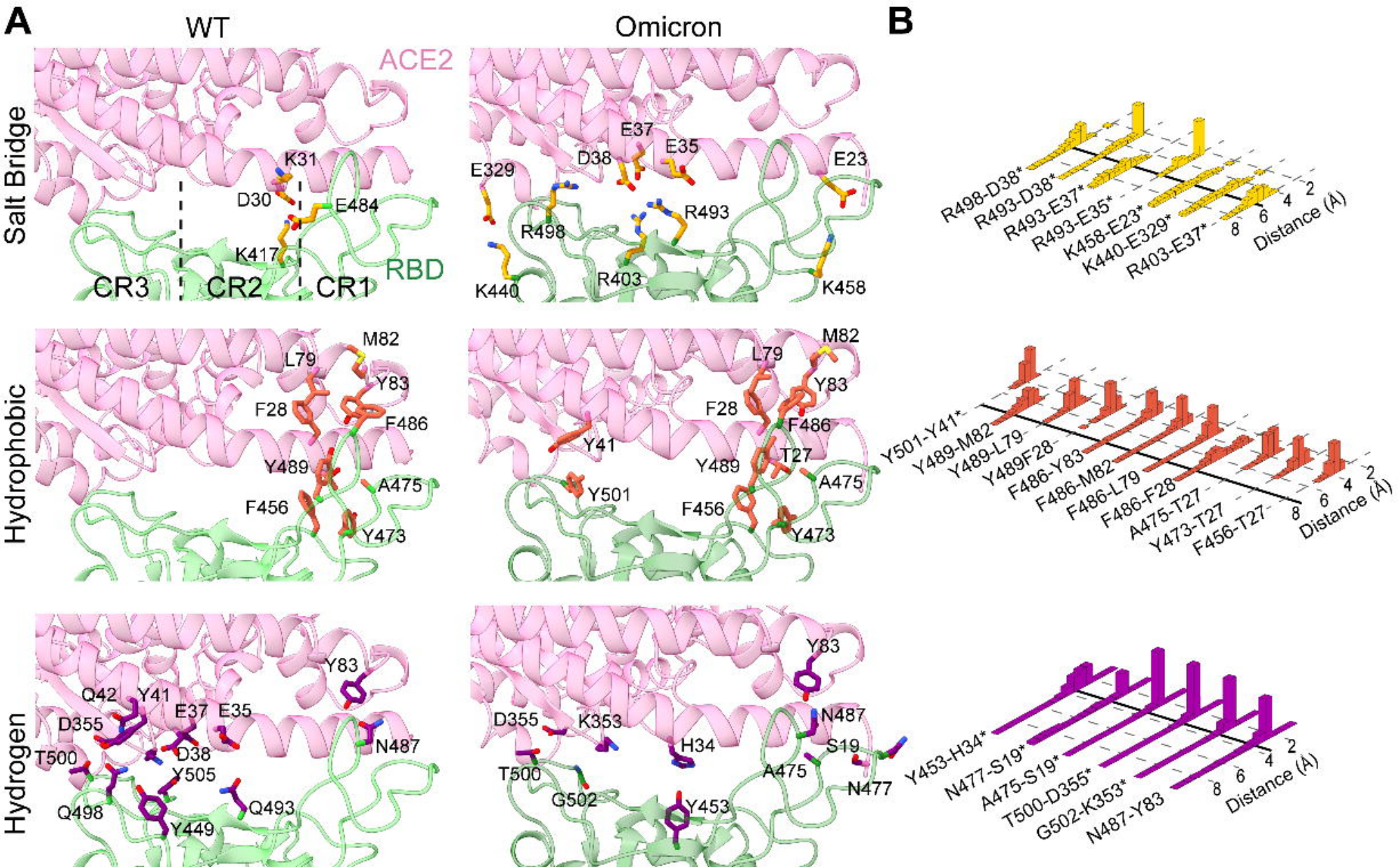
A
WT
Omicron
B
Salt Bridge
Hydrophobic
Hydrogen
ACE2
RBD
CR3
CR2
CR1
K31
D30
E484
K417
E37
D38
E35
E23
E329
R493
R498
K440
R403
K458
M82
L79
Y83
F28
F486
Y489
A475
F456
Y473
Y41
Y501
T27
Y83
Q42
Y41
E37
E35
D355
D38
N487
T500
Y505
Q498
Q493
Y449
K353
H34
S19
A475
N477
G502
Y453
R498-D38*
R493-D38*
R493-E37*
R493-E35*
K458-E23*
K440-E329*
R403-E37*
Y501-Y41*
Y489-M82
Y489-L79
Y489F28
F486-Y83
F486-M82
F486-L79
F486-F28
A475-T27
Y473-T27
F456-T27
Y453-H34*
N477-S19*
A475-S19*
T500-D355*
G502-K353*
N487-Y83
8
6
4
2
Distance (Å)